Supporting Information for

Solution-Fabricated Tellurium/Silicon mixed-dimensional van der Waals Heterojunction for Self-Powered Photodetector

Tao Zheng[a,b,§], Mengmeng Yang[c,§], Yiming Sun[a,b], Lixiang Han[a], Yuan Pan[a,b], Qixiao Zhao[a,b], Zhaoqiang Zheng[c], Nengjie Huo[a,b], Wei Gao[a,b*] and Jingbo Li[a,b*]

[a] Institute of Semiconductors, South China Normal University, Guangzhou 510631, P. R. China

[b] Guangdong Provincial Key Laboratory of Chip and Integration Technology, Guangzhou 510631, China

[c] School of Materials and Energy, Guangdong University of Technology, Guangzhou 510006, P. R. China.

Corresponding authors: Wei Gao, Email: gaowei317040@m.scnu.edu.cn Jingbo Li, Email: jbli@m.scnu.edu.cn

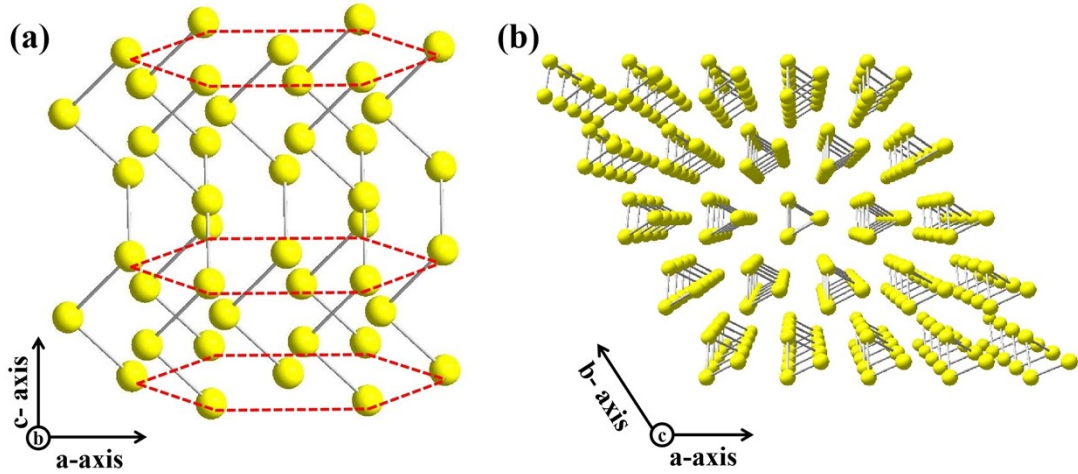[§]These authors contributed equally to this work.

Figure S1 The lattice structure of 2D Te nanosheet. (a) the b-axis views and (b) the c-axis views of Te atomic structure.
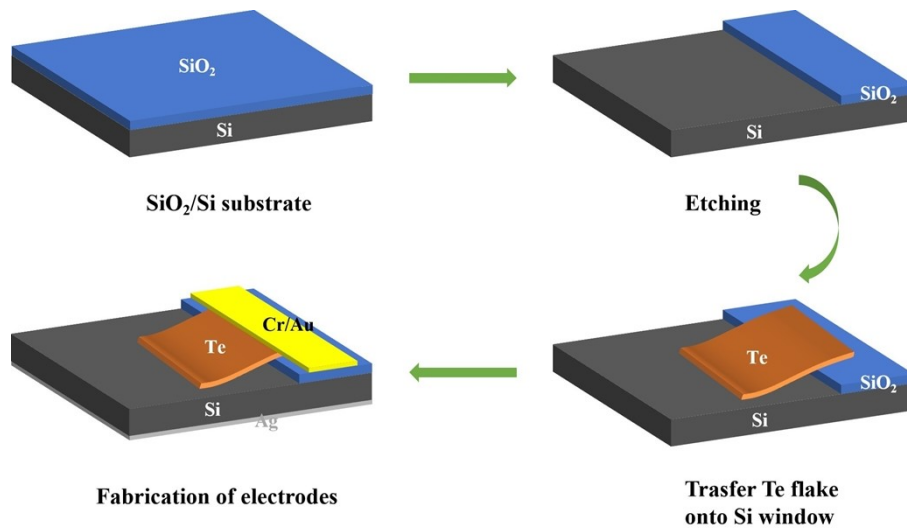

Figure S2 Schematic illustration for the fabrication process of Te/Si van der Waals heterojunction photodiode.
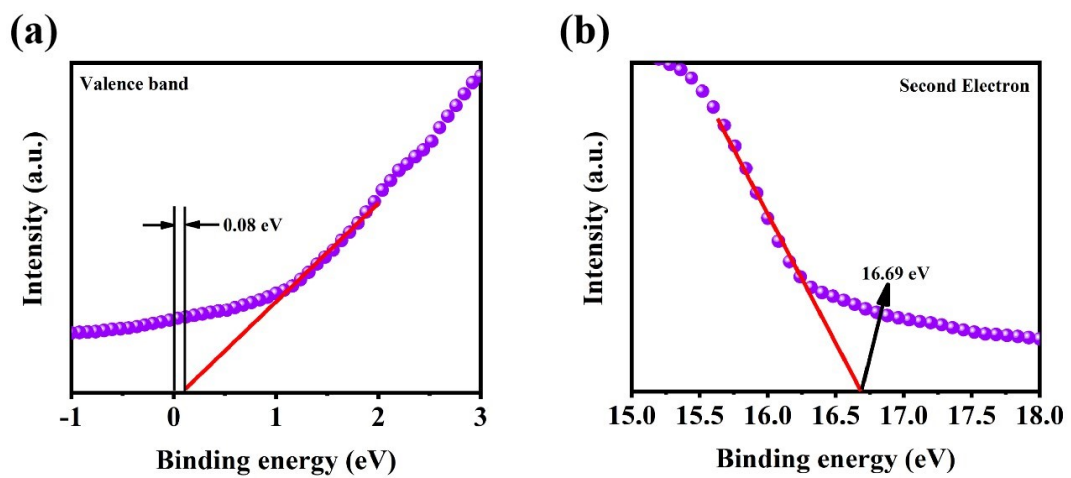

Figure S3 UPS spectra of Te samples displaying (a) the valence band spectra and (b) second electron

cutoffs.

The UPS spectra are utilized to confirm the valence band and work function of Te. The work functions of Te was estimated to be 4.51 eV, according to $W = h\nu - E_{cut}$, where $h\nu$ = 21.2 eV is the photon energy of He I light source. The valence band edges of Te was 0.08, lower than its Fermi level (binding energy equals to 0 eV).
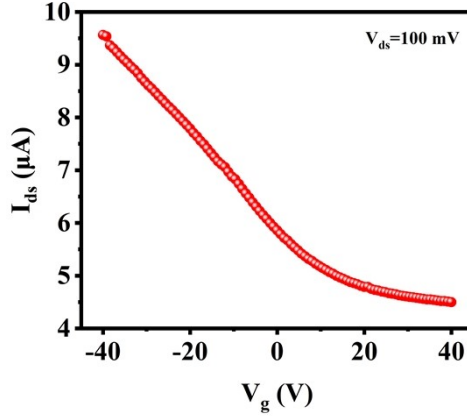

Figure S4 The transfer curve of the Te-based field effect transistor.

This device was prepared as follows: The as-grown Te nanosheet with the similar thickness as Te nanosheet in the heterojunction device was firstly transferred onto the commercially purchased p-type heavily-doped Si/SiO_2 (300 nm) substrate. Next, 10 nm Cr/50 nm Au was successively deposited by photolithography, electron beam evaporation, and lift-off process. The hole mobility can be calculated by the following formula[1]: $\mu = \frac{\partial I_{ds}}{\partial V_g}(\frac{Ld}{W\varepsilon_0\varepsilon_r V_{ds}})$ where μ is mobility, $\frac{\partial I_{ds}}{\partial V_g}$ is slope of the typical transfer curve, L and W are the length and width of the channel, d is the thickness of the SiO_2 layer, ε_0 is the electric constant, and ε_r is the relative static permittivity. Here, V_{ds} = 0.1 V, L = 5 μm, W = 3 μm, d = 300 nm, ε_0 = 8.85 × 10⁻¹² F/m and ε_r =3.9. Based on the data shown in Figure S1, $\frac{\partial I_{ds}}{\partial V_g}$ = 1 × 10⁻⁷ A/V. Then,

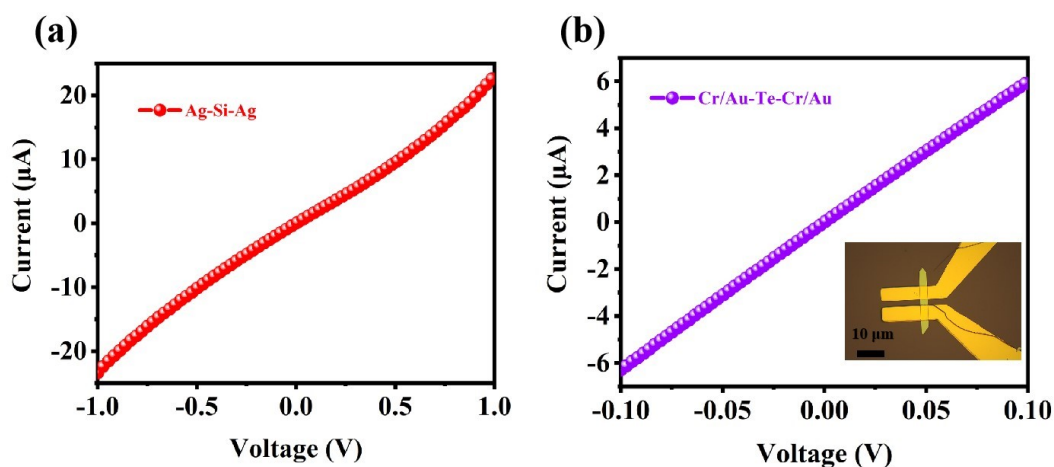the field-effect hole mobility is calculated to be 141 $cm^2\,V^{-1}\,s^{-1}$.

Figure S5 The I-V curves of (a) Ag-Si-Ag and (b) Cr/Au-Te-Cr/Au measured at room temperature in dark, the inset shows an optical image of the Te-based transistor.

The conductivity can be calculated by the following formula[2]: $\sigma = \dfrac{1}{\rho} = \dfrac{L}{RS}$) where μ

is conductivity, L and S are the length and cross-section area of the channel, R is the resistance of the Te nanosheet. Here, $L = 5$ μm, $S = 0.24$ μm^2, $R = 16$ KΩ which can be obtained from the I-V curve in Figure S4b. Then, the conductivity is calculated to be 13 S/cm.
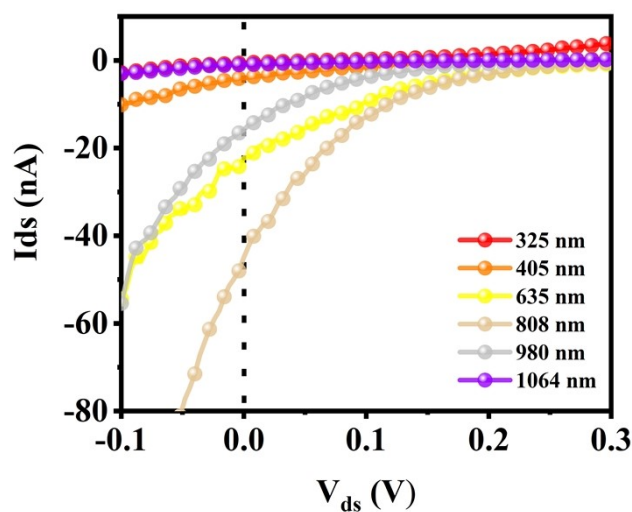

Figure S6 I-Vcurves with photovoltaic behaviours of the device under light illumination with different
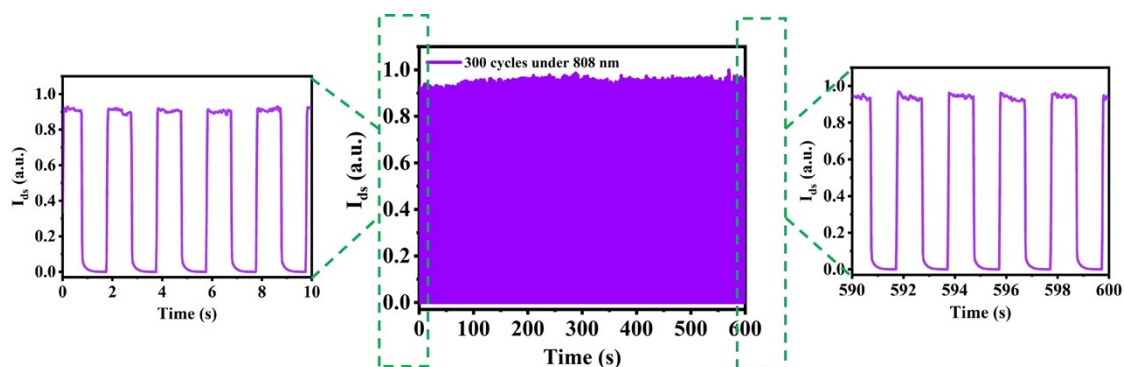
wavelengths.

Figure S7 Time-dependent photoresponse of the photodiodes for 300 cycles, and the inner diagrams on the left and right sides show the start and end of the test as a magnified view of the response curve.
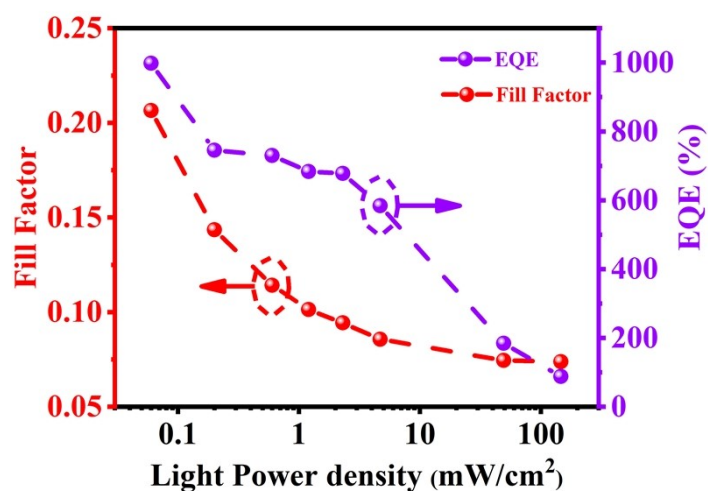

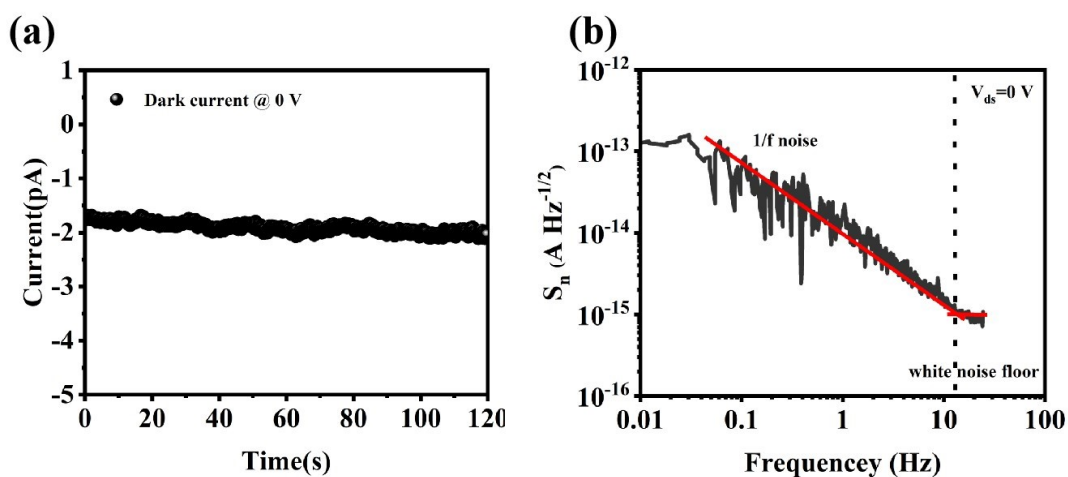**Figure S8** Fill Factor and EQE as a function of light power density of under 808 nm.

Figure S9 (a) Dark current and (b) the noise spectral density of the Te/Si vdWH device recorded at 0 V bias voltage.
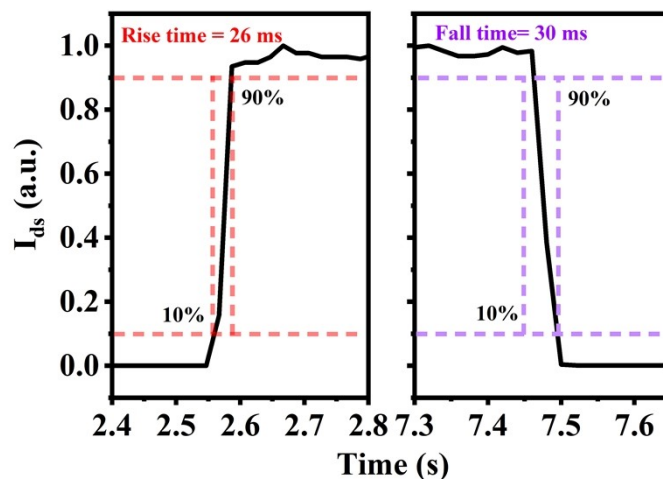
Figure S10 Rise and decay time in One cycle of the photoresponse curve.
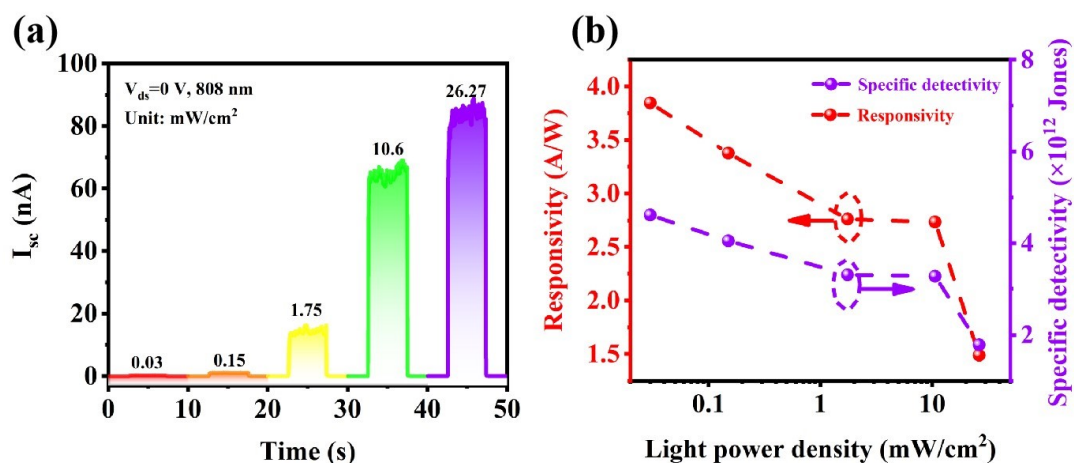

Figure S11 (a) The real-time photoresponse properties of the Te/Si vdWH device under the light illumination of 635 nm at different light power densities under zero bias voltage. (b) The corresponding responsivity and specific detectivity dependent on light power density under the illumination of 635 nm.

Supporting Reference

1. W. Gao, Z. Zheng, L. Huang, J. Yao, Y. Zhao, Y. Xiao and J. Li, Acs Appl. Mater. Inter., 2019, 11, 40222-40231.

2. Q. Yue, W. Gao, P. Wen, Q. Chen, M. Yang, Z. Zheng, D. Luo, N. Huo, F. Zhang, and J. Li, J. Mater. Chem. C, 2021, 9, 15662-15670.